ACS Catalysis

Research Article

pubs.acs.org/acscatalysis

Dominant Influence of the Surface on the Photoactivity of Shape-Controlled Anatase TiO_2 Nanocrystals

Xiaomei Yu, Byungwook Jeon, and Yu Kwon Kim*

Department of Energy Systems Research and Department of Chemistry, Ajou University, Suwon 443-749, South Korea

ABSTRACT: Shape-controlled anatase TiO_2 nanocrystals with large {001} facets are synthesized by a hydrothermal method using HF as a shape-controlling agent. The photoactivity of the TiO_2 nanocrystals is evaluated from the photodegradation rate of methylene blue in aqueous solution under UV irradiation. Here, we observe higher photoactivities for the TiO_2 nanocrystals with a {001} ratio of close to 60%, which is the shape effect in photoactivity. In addition, we observe that the photoactivity is further enhanced when the TiO_2 nanocrystals are treated in a dilute NaOH (HF) solution. Our SEM, XPS, and EPR analyses reveal that the etching in the NaOH (HF) solution can induce significant changes in the surface defects as well as in the surface morphology. We find that the enhanced photoactivity is closely related to the changes in the surface defects, which favor the formation of surface O^- species under ambient conditions.

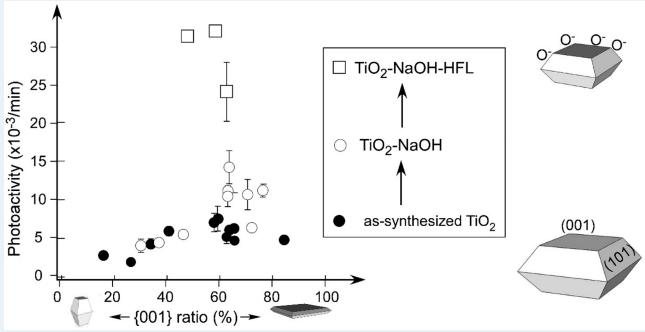

KEYWORDS: *anatase TiO_2 nanocrystal, photoactivity, shape effect, surface effect*

INTRODUCTION

Among various oxide nanocrystals, anatase TiO_2 nanocrystals have drawn a great deal of attention because of their potential use in applications such as photocatalysis, photovoltaic cells, and sensors.[1,2] TiO_2 is a chemically stable nontoxic semiconductor with a wide band gap (3.2 eV) that absorbs UV light, which induces photogenerated hot carriers. They need to be separated in order to be utilized in applications such as photodegradation, photovoltaics, and photocatalytic water splitting.[3]

To enhance the photoresponsive capability in such applications, research efforts have been made in controlling the shape of oxide nanocrystals, since their reactivity is strongly dependent on the detailed atomic structure of various exposed facets.[4−8] Recently, the high photocatalytic activity of {001} facets of anatase TiO_2 nanocrystals has been recognized in various reactions and many efforts have been made to synthesize anatase TiO_2 with a large percentage of exposed {001} facets.[9−13]

Normally, anatase TiO_2 nanocrystals favor {101} facets due to the low surface energy (0.44 J/m^2); it results in a crystal shape of a truncated tetragonal bipyramid with large {101} facets. The {001} facets are largely avoided due to the high surface free energy (0.9 J/m^2). This thermodynamic tendency can be tuned by controlling the relative surface free energy of various facets such as {101} and {001}: for example, by using fluorine ions as surfactants.[14] This approach has been proven to provide a way of producing TiO_2 nanocrystals with varying {001} ratios of 27−89%.[15−19]

On the basis of such a tunability in shape, there are increasing reports suggesting a close relation between the exposed facets and the overall photoactivity.[1,7,9,11,14,16,18,20−41] Interestingly, the relation is revealed to be even more complicated than a simple proportionality of photoactivity to the exposed area of reactive facets.[24,25,30,35,36,42,43] The crystals with large reactive facets such as {001} generally show a higher photoactivity.[17] However, there are also reports showing a higher photoactivity of TiO_2 nanocrystals with lower {001} ratios.[24] In some cases, the reactive {001} facets are reported to show a lower photoactivity than {101} facets.[25] The shape-dependent photoactivity of anatase TiO_2 nanocrystals is also proposed to be the result of a cooperative role of {001} and {101} facets in separating photogenerated electrons and holes, which is inferred from a higher photoactivity of TiO_2 nanocrystals with a lower {001} ratio (45%) in comparison to that of TiO_2 nanosheets with a higher {001} ratio (82%).[43]

The shape effect is further complicated by uncontrolled contribution from various surface species, such as surface defects and F ions. Oxygen-deficient TiO_2 nanosheets[7] have been reported to show higher photoactivities in comparison to the TiO_2 nanocrystals with negligible defects which are obtained after annealing up to 600 °C; this procedure can influence the overall shape of the nanocrystals and crystallinity as well. In addition, the F ions used as surfactants can be left on the TiO_2 surfaces and have strong influences on photoactivity, even though the exact role of F is still controversial. Photocatalytic H_2 production is reported to be enhanced in the presence of F species on the surface when Pt is used as a

Received: December 26, 2014
Revised: April 20, 2015
Published: April 20, 2015

DOI: 10.1021/cs5020942
ACS Catal. 2015, 5, 3316−3322

cocatalyst.[23,44] The enhanced photoactivity of F-TiO_2 is attributed to a facile formation rate of $^{\bullet}OH$ radicals in the presence of F.[18,45] However, there are also contradicting reports of enhanced photoactivity when F is removed from the surface.[17,24]

Thus, despite such a large number of reports on the issue of shape-dependent photoactivity, there are still questions of what the origin of the shape-dependent photoactivity is and how it is influenced by the presence of surface species such as F. The influence of F on the photoactivity may depend on the shape of TiO_2 nanocrystals.

Here, we present a quantitative investigation into the shape-dependent photoactivity of TiO_2 nanocrystals prepared with varying amounts of HF, which have remanent F species on the surface. To understand the effect of such remanent F species on the photoactivity, the photoactivity measurements have been carried out before and after the removal of such F species by a treatment in aqueous NaOH solution. In addition, the nanocrystals have been further treated with HF to confirm the effect of surface F species.[44]

Our results suggest that the photoactivity of the TiO_2 nanocrystals with an {001} ratio of ~60% is generally enhanced in comparison to that of others; this stresses the importance of the crystal shape, which explains the effect of neighboring facets.[41,46] In addition, the subsequent NaOH (HF) treatment further enhances the photoactivity. In particular, long HF treatments (~3 h) turn out to enhance the photoactivity even further. Our detailed analyses described in the Results and Discussion strongly suggest additional roles played by the surface defects as well as the surface morphology determined by the NaOH/HF treatments.

EXPERIMENTAL DETAILS

Synthesis of Anatase TiO_2 Nanocrystals (TiO_2−HF*x*). A hydrothermal method was employed for the synthesis of anatase TiO_2 nanocrystals. A 25 mL portion of butanol and 25 g of tetrabutyltitanate (TBT) were placed in a Teflon beaker in an ice bath. Varying amounts (0−12 mL) of a concentrated HF aqueous solution (48 wt %) was subsequently placed in the beaker in a dropwise manner with vigorous magnetic stirring. The resulting homogeneous solution was then transferred into an autoclave which was placed in an oven maintained at 200 °C for 24 h. White precipitates were collected from the autoclave by filtration, rinsed with deinonized water several times, and finally dried at 80 °C. The resulting as-synthesized TiO_2 powders are labeled as TiO_2−HF*x*, in which *x* indicates the amount of HF used.

NaOH Treatment of TiO_2 Nanocrystals (TiO_2−NaOH). A 1.0 g portion of as-synthesized TiO_2 powder was dispersed in 0.1 M NaOH solution. The solution was magnetically stirred for a few hours at room temperature.[47] After the treatment, the TiO_2 powder was recovered by centrifugation, washed with deionized water and ethanol several times, and finally dried at 80 °C for 6 h.

HF Treatment of TiO_2 Nanocrystals (TiO_2−NaOH−HF). A 0.5 g portion of NaOH-treated TiO_2 powder was dispersed in 5 wt % HF aqueous solution, and the solution was magnetically stirred for 1/2 h (TiO_2−NaOH−HFs) and 3 h (TiO_2−NaOH−HFL) at room temperature, respectively.[44] After the treatment, the TiO_2 powder was recovered by centrifugation, washed with deionized water and ethanol several times, and finally dried at 80 °C for 6 h.

Characterization of TiO_2. The shape and morphology of as-synthesized TiO_2 (TiO_2−HF*x*) were evaluated by observing scanning electronic microscopy (SEM) images. The X-ray diffraction (XRD) spectra were obtained from an X-ray diffractometer (Rigaku, Ultima III) using Cu Kα radiation (λ = 0.15406 nm) to examine the bulk phase of the TiO_2 nanocrystals. Electron paramagnetic resonance (EPR) spectra were taken from JES-TE200 (JEOL) by applying an X-band (9.43 GHz, 1.5 mW) microwave and sweeping magnetic field at room temperature. X-ray photoelectron spectroscopy (XPS) measurements were performed with an XPS system (PHI, 5000 VersaProbe II) with Mg Kα radiation (1253.6 eV) and a charge neutralization system. All of the binding energies were referenced to the C 1s peak at 284.4 eV of the surface adventitious carbon.

Photoactivity Measurements. Photo-oxidation of methylene blue (MB) under UV light irradiation (15 W, 365 nm) was performed in an aqueous solution of MB (0.01 mM) with TiO_2 nanocrystals (0.006 g/L) suspended in it, respectively. Under our reaction conditions, the pH was maintained within 5−6 throughout the whole measurement. The resulting photoactivity was evaluated by measuring the initial first-order rate constant in units of min^{-1}, while the initial concentrations of MB and TiO_2 were fixed. In general, the photoreaction rate in the liquid phase does not increase in proportion to the exposed surface area because it is influenced by number of factors, such as light absorption (which can be strongly influenced by scattering by particles), charge carrier generation, and subsequent migration.[48] Before the measurement, the solution was magnetically stirred for 1 h in a dark place to achieve an equilibrium. The initial photodegradation rates were measured at room temperature from a decrease in the absorbance at 665 nm in the absorption spectrum. The measurement conditions allowed us to assume that the influence of reaction products and any possible structural changes in TiO_2 are negligible. After the photoreaction, the TiO_2 crystals were found to preserve their shape as well as their bulk phase under our reaction conditions, as determined from SEM and XRD measurements. Up to five measurements were performed for each rate constant to avoid any uncontrolled uncertainty associated with reaction conditions.

RESULTS AND DISCUSSION

The SEM images of as-synthesized TiO_2 nanocrystals shown in Figure 1 exhibit nanosheet-like shapes, especially for HF2−

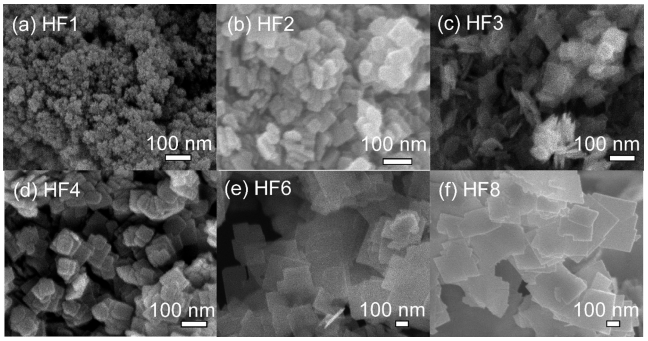

Figure 1. SEM images of as-synthesized anatase TiO_2 (TiO_2−HF*x*) with varying amounts of HF (1−8 mL): (a) TiO_2−HF1; (b) TiO_2−HF2; (c) TiO_2−HF3; (d) TiO_2−HF4; (e) TiO_2−HF6; (f) TiO_2−HF8.

DOI: 10.1021/cs5020942
ACS Catal. 2015, 5, 3316−3322

HF4. The shapes of our TiO_2 nanocrystals are truncated tetragonal bipyramids with {001} and {101} facets, as determined in our previous report.[49] The average size of the {001} facets increases with increasing HF (up to HF4) within 50−100 nm. The thickness is estimated to be in the range 5−20 nm with a trend of increasing thickness when a lower amount of HF is used; when the average size of {001} facets increases from 50 to 100 nm, the thickness is reduced from ∼20 to 10 nm. At higher HF (HF6−HF8), nanosheets with much larger {001} facets (>200 nm) are obtained. When the amount of HF used is 1 mL (TiO_2−HF1) or lower, smaller TiO_2 nanoparticles 10−20 nm in size are obtained in a form of aggregates.

On the basis of the SEM observations, the ratio of {001} facets to others such as {101} can be estimated by assuming the truncated-tetragonal-bipyramidal shape. The {001} ratio of our TiO_2 nanocrystals (HF0−HF8) is found to increase from 30 for HF1.5 to 60% for HF3. The ratio further increases up to 90% for HF8. The size distribution is estimated to be within ±10% of the mean value. That is, the {001} ratio of the TiO_2−HF2 nanocrystals is estimated to be ∼52 ± 10%.

XRD measurements in Figure 2 indicate that all of the TiO_2 nanocrystals are in the anatase phase with a fairly good

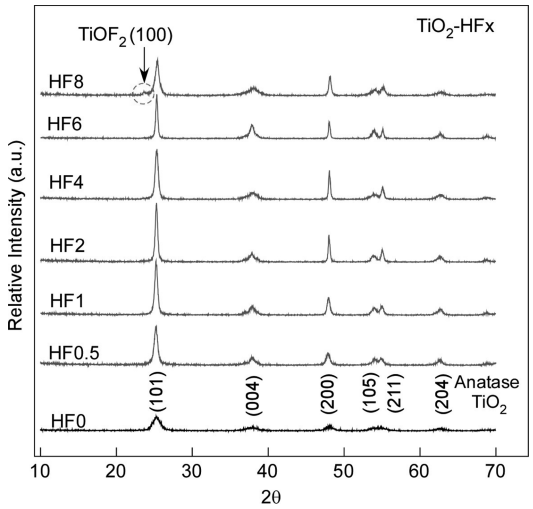

Figure 2. XRD patterns of TiO_2 nanocrystals (TiO_2−HF*x*) synthesized with varying amount of HF (0−8 mL), showing anatase phase with a good crystallinity.

crystallinity, except for TiO_2−HF0. When HF is not used, broad XRD peaks indicate that the average size of the TiO_2 nanocrystals is about 7 nm, as determined from full width at half-maximum (fwhm) of the (101) peak. When an excess amount of HF (∼8 mL or higher) is used, evidence for the formation of a F-derived phase such as $TiOF_2$ is found in addition to the anatase TiO_2 phase. In all other cases (0 < HF < 8 mL), only the anatase phase is observed in XRD with sharp peaks. The intensity of the (200) peak increases with increasing HF up to 4 mL, and then it decreases at higher HF. The increased intensity of the (200) peak reflects the increase of the {001} facet. In addition, the width of the (004) peak reflects the variation of the thickness of the nanosheets. The average value of the {001} ratio can be obtained from the XRD peak intensities of the (004) and (200) peaks.[15,50,51] The calculated ratios are employed in Figure 3 to show the shape-dependent photoactivity.

From the results of Figures 1 and 2, we confirm that crystalline anatase TiO_2 nanosheets with a fairly good size distribution are obtained with 2−4 mL of HF under our experimental conditions.

The photoactivity of our anatase TiO_2 nanosheets prepared with HF is compared in Figure 3. Here, the effect of shape or

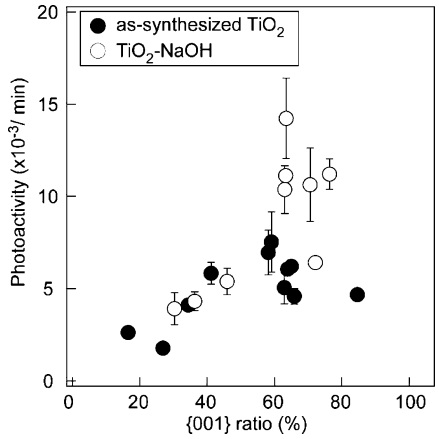

Figure 3. Photoactivity of as-synthesized anatase TiO_2 nanocrystals (TiO_2−HF*x*) before and after the NaOH treatment plotted against the {001} ratio determined from the XRD peak intensity ratio in Figure 2.

the dependence of photoactivity on the ratio of the {001} facet is shown by plotting the rate constants (*k*) obtained from the as-synthesized TiO_2 and those after NaOH treatments against the {001} ratio determined from the XRD spectra in Figure 2. The thickness along the [001] direction and the average length along the [100] direction can be obtained from the fwhm value of (004) and (200) Bragg peaks. The percent ratio of exposed {001} facets is calculated by assuming that the nanosheets are in the shape of truncated tetragonal bipyramids.[50]

Despite an irregularity of about ±10% in the {001} ratio of our TiO_2 nanocrystals, Figure 3 shows a clear trend of enhanced reaction rate at a {001} ratio of ∼60%. A higher photoactivity of up to 9×10^{-3}/min is measured for TiO_2 with an {001} ratio of ∼60%, while a lower photoactivity close to 4×10^{-3}/min is obtained when the {001} ratio deviates from 60%.

The enhanced photoactivities of anatase TiO_2 nanosheets prepared with HF (HF2−HF4) are often attributed to a better crystallinity and the existence of a well-defined reactive facet[41] such as {001}.[52] In addition, the interplay between neighboring facets of {001} and {101} is also suggested to be beneficial in an efficient separation of charge carriers,[41,46] which results in an enhanced photocatalytic activity; the two neighboring facets possessing different reaction sites for photo-oxidation and reduction,[28] respectively, may draw holes and electrons to the respective facets separately and inhibit the recombination of photogenerated charge carriers, leading to an enhanced photoactivity.

Figure 3 also shows the photoactivity of the TiO_2 nanocrystals after the NaOH treatment which may eliminate surface fluorine. We find that the peak widths of (004) and (200) change slightly after prolonged NaOH treatments, indicating a possible change in shape. The {001} ratios determined from XRD indicate that the ratio of 60−65% can be shifted up to 65−75% after the NaOH treatments. This may be related to changes in surface morphology, as will be discussed later. However, when the treatment time is 10 min, the {001}

DOI: 10.1021/cs5020942
ACS Catal. 2015, 5, 3316−3322

ratio is maintained within ±1%. Since the NaOH treatment is performed at room temperature, only the surface (not the bulk) of the nanocrystals can be assumed to be influenced. In Figure 3, we find that the effect of the surface treatment by NaOH is to enhance the photoactivity up to ∼15 × 10^{-3}/min. It is interesting to note that such an enhanced photoactivity after the NaOH treatment occurs only for those nanocrystals with a {001} ratio of 60−70%, while the enhancement is not obvious for those with a lower {001} ratio (<50%). The shape-dependent effect of NaOH treatments on photoactivity among TiO_2 nanocrystals with different {001} ratios may be related to the removal of F from the {001} facets by OH.[53] Since the remenant F concentration would be lower on TiO_2 nanocrystals with lower {001} ratios, the effect of the NaOH treatment (that is, removal of F) can be marginal, as observed in Figure 3. The NaOH treatment may also induce changes in the surface morphology, including step density and point defects. Such changes could have an influence on the photoactivity after the NaOH treatment, as shown in Figure 4.

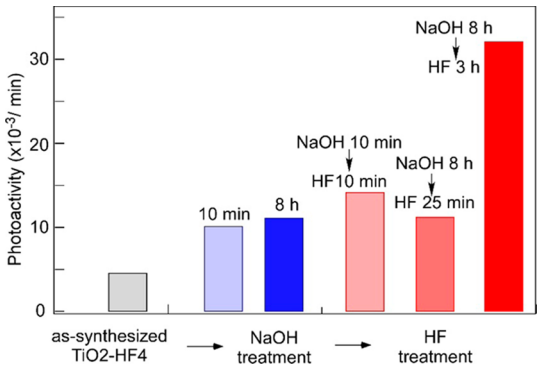

Figure 4. Photoactivity of as-synthesized TiO_2−HF4 in comparison with those after the NaOH treatments (TiO_2−NaOH) for 10 min and 8 h, respectively as well as after the subsequent HF treatments for 10 min, 30 min (TiO_2−NaOH-HFs) and 3 h (TiO_2−NaOH-HFL), respectively.

The surface treatment-induced variation in photoactivity is further examined in Figure 4. Here, we show that the NaOH treatment can induce an enhancement in photoactivity regardless of treatment time (10 min, 8 h). To understand the origin of the enhancement induced by the NaOH treatment, the NaOH-treated TiO_2 has been further treated with HF to fluorinate the surface. We find that the TiO_2 nanocrystals treated with HF for a short time (10 and 30 min) show about the same photoactivity as that of TiO_2−NaOH, while a long HF treatment (3 h) induces an approximately 3 times additional enhancement in photoactivity. The successive treatments of NaOH and HF were also performed with other TiO_2 samples (TiO_2−HF2 and TiO_2−HF3) with similar {001} ratios, and the results are found to show a very similar trend. Since all the treatments would only affect the surface, all of the variations in photoactivity should be related to changes in the surface species such as surface defects in addition to the possible changes in the surface F concentration, as well as in the surface morphology. It is rather surprising that we obtain very similar enhancement in photoactivity after successive treatments of NaOH and HF (Figure 4), since the NaOH (HF) treatment is expected to decrease (increase) surface F content, which can have a strong influence on photoactivity. This may be because the absolute F content is low and the variation of it due to the NaOH (HF) treatment is less important than any other surface defects that can be present on the surface. Factors such as the surface morphology and the variation of other kinds of surface defects upon the surface treatments may be more likely to play a role in the observed enhancement in photoactivity.

Figure 5 shows SEM images of TiO_2−HF4 after successive treatments in NaOH and HF, respectively. We find that the

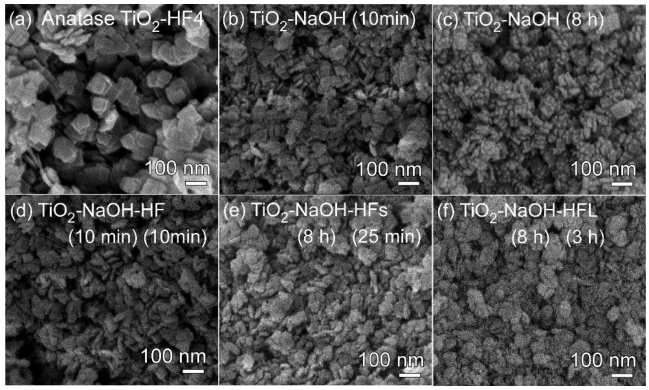

Figure 5. SEM images of as-synthesized and surface-modified TiO_2−HF4 samples: as-synthesized TiO_2 (a), after NaOH treatments for 10 min (b) and 8 h (c), and after subsequent HF treatments for 10 min (d), 25 min (e), and 3 h (f).

overall size and shape of our TiO_2 nanocrystals are maintained after the NaOH treatment for 10 min (Figure 5b) as well as after the HF treatment for 10 min (Figure 5d). XRD measurements also indicate that the {001} ratio of TiO_2−HF4 (∼60%) is maintained to be the same within ±1% after a 10 min HF(or NaOH) treatment. After the NaOH treatment for 8 h (Figure 5c), however, we find that the facets of TiO_2 are decorated with small granules, which are considered to be a result of etching and recrystallization of the surface layers in the aqueous NaOH solution. As a result, the {001} ratio of TiO_2 (60−65%) is measured to be shifted up to 65−75%. After a subsequent HF treatment for 0.5 h (Figure 5e), the small granules on the surface are removed and rather smooth surfaces reappear. A long (3 h) HF treatment (Figure 5f) still leaves the crystal shape of the nanosheet maintained, but with a smaller size. This is the result of an etching of the surface layers of TiO_2 nanocrystals by HF.[54] Here, the {001} ratio is measured to be close to that of as-synthesized TiO_2, especially for those with a ratio close to ∼60%. The amount of TiO_2 removed in the HF solution during the long HF treatment is estimated to be about ∼40% of the initial weight. Further evidence on the possible changes in the surface composition and structure are provided and discussed in the XPS (Figure 6) and EPR (Figure 7) spectra.

The changes in the surface F content are monitored by XPS as shown in Figure 6. The O 1s and Ti 2p core levels confirm that a stoichiometric amount of TiO_2 is maintained after the successive treatments. A single Ti $2p_{3/2}$ peak at 459 eV without any low binding feature is observed after all successive treatments. In addition to Ti and O, no other chemical species except for F is detected. We find a single F 1s peak at ∼685 eV from as-synthesized TiO_2 nanosheets. The F ions which act as surfactants are strongly bound to the surface of TiO_2 nanosheets by forming a Ti−F bond[7,15,16] when TiO_2 nanocrystals are prepared with HF. This peak intensity

DOI: 10.1021/cs5020942
ACS Catal. 2015, 5, 3316−3322

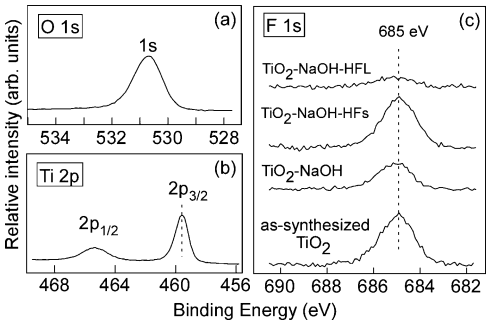

Figure 6. O 1s (a) and Ti 2p (b) XPS spectra of as-synthesized TiO_2−HF4. (c) F 1s XPS spectra of as-synthesized and surface-modified TiO_2−HF4 samples.

decreases after the NaOH treatment due to the removal of surface F (Figure 6c).[17,44] The remanent F peak reflects the existence of surface F species in the TiO_2 nanosheets due to an incomplete removal of surface F or may come from F species incorporated into the bulk. Without any doubt, the subsequent HF treatment induces the binding of more F on the surface, as can be confirmed from Figure 6c. The atomic percentage of F determined from the XPS intensity with sensitivity correction is ∼3% after the NaOH treatment, which can be compared to 6−7% of as-synthesized (or HF treated) TiO_2. Interestingly, the F 1s peak intensity decreases drastically after the long HF treatment. This elimination of surface F (down to <1%) is likely to be the result of etching of surface Ti species by F as TiF_6^{2-}. This process would consume F ions in the aqueous solution, thus diluting the F concentration. The number of F ions in the HF solution used is estimated to be about 10 times the total number of Ti atoms in TiO_2. Thus, there would be excess F ions surrounding the TiO_2 nanocrystals after etching for 3 h in the HF solution. As the etching continues, however, excess fluorinated Ti species in the aqueous phase are also expected to be populated in the solution and are in competition with these F ions for binding to the surface of TiO_2 nanocrystals. In addition, incompletely solvated Ti species would interact rather strongly with the surface, which may inhibit the binding of F ion to the TiO_2 surface. Such Ti species may be removed during washing. This may be the origin of such dramatic reduction of surface F species after a long HF treatment.

Combining the results in Figure 4 and Figure 6, it is clear that the absolute F content alone on the surface has no direct effect on the measured photoactivity in our case; the photoactivities of the NaOH-treated and HF-treated TiO_2 are very similar to each other even though the F content is different. In addition, a comparison of the photoactivities of the as-synthesized TiO_2 and the HF-treated TiO_2 ($aTiO_2$−HFs) shows that the photoactivity is different even though the F content is about the same (∼6−7%) on the surface. A strongly enhanced photoactivity is observed for the HF-treated TiO_2 for a long time, which has very low F content on the surface.

Instead, the detailed changes in the surface morphology, including the type and the density of defects, are likely to be responsible for the observed changes in the photoactivity of our anatase TiO_2 nanocrystals.

Any evidence of variation in the type of surface defects and their concentration can be obtained from a change in the EPR signal after the successive treatments in aqueous solution of NaOH and HF, respectively; under such a room-temperature treatment in aqueous solution, any change in the EPR spectra is likely to be induced by changes on the surface, not in the bulk. EPR spectra in Figure 7 show a meaningful change in the EPR

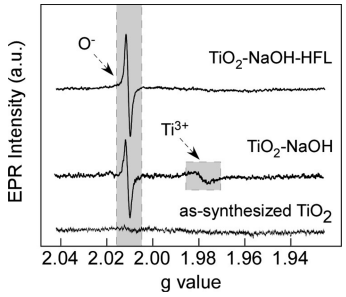

Figure 7. EPR spectra of as-synthesized and surface-treated TiO_2−HF4 nanocrystals.

signals, suggesting a change in the surface defects after the treatments. Since F is present on the surface of TiO_2 (Figure 6), one may expect a characteristic EPR signal of F (g = 1.97)[7,55] if F is incorporated into lattice of TiO_2, as has been found for F-doped TiO_2[56] prepared by the sol−gel method. However, no such EPR signal is detected from all our as-synthesized TiO_2−HFx nanocrystals. Thus, we conclude that F species observed in XPS (Figure 6) are present only on the surface, not in the bulk. A trace of a single peak at g = 2.01 is attributed to O^- species; this is observed to be pronounced especially for TiO_2−HFx with x < 2 (not shown here).

Although there is no pronounced EPR signal observed from TiO_2−HFx with x = 2−4, clear signals appear at g = 2.01 and 1.98 after the NaOH treatment, which are indicative of a formation of O^- and Ti^{3+} species,[57−60] respectively, on the surface. After the subsequent treatment in HF, only the peak at g = 2.01 remains. We also observe the same EPR signal after the HF (NaOH) treatment for only 10 min as well. The absolute intensity is quite lower than that for longer treatments; the magnitude of the O^- signal is not linearly related to the enhancement in photoactivity observed in Figure 4. In addition, the EPR measurement is performed from the TiO_2 nanocrystals under ambient conditions at atmospheric pressure, not in an aqueous solution. Thus, the O^- species may not exist at all in an aqueous solution under photoreaction conditions. However, the observation of the O^- species on TiO_2 implies the presence of surface defect sites which can accommodate O_2 and dissociate it into O^-. During the photocatalytic reaction in aqueous solution, the presence of such surface defects can attract charge carriers, leading to a net separation of photogenerated electrons/holes.

It is also worth mentioning that the photoactivity of NaOH-treated TiO_2 (Figure 4) is about the same regardless of the treatment time (10 min and 8 h), while the surface morphology (Figure 5) is significantly different between the two. Both surfaces show an O^- signal in EPR, but with lower intensity for 10 min. This again suggests that the O^- species itself (observed in EPR) is not an immediate cause of the enhanced photoactivity. In addition, the absolute intensity of the EPR signal may change even for the same TiO_2, depending on whether it is dried at elevated temperature (∼100 °C) or is left under humid conditions.

Even though our observation of O^- species may not be an immediate measure of defects responsible for enhanced photoactivity, it may be inferred that the existence of such

DOI: 10.1021/cs5020942
ACS Catal. 2015, 5, 3316−3322

O^- species can be a strong indication that certain types of surface defects, which can induce O^- species, become populated after the NaOH (HF) treatment and have a decisive effect on the photoactivity, instead of detailed surface morphology.

Our results also stress the importance of the type of facets of TiO_2 in the defect-induced enhancement of photoactivity, since we observe the enhancement especially when the {001} ratio is close to 60%. The role of facets is important, since the formation of surface defects would be dependent on the types of facets. The fact that there is an optimum ratio for the treatment-induced enhancement also explains the cooperative role of different facets (with different types and concentrations of surface defects) possibly in the efficient charge separation.

Combining our results, it is likely that the contradicting reports[17,18,23,24,44,45] on the role of surface F and the effect of NaOH treatment may originate from the varying contribution of surface defects and the degree of surface roughness, which are largely uncontrolled factors in many experiments performed in an aqueous solution. Thus, it is imperative to evaluate the surface morphology and surface defects to understand the origin of photoactivity of TiO_2 nanocrystals. The detailed roles of surface F species and the surface defects (including surface O^- species) may vary depending on the kind of photoreactions evaluated. In our case, the existence of surface O^- species on the TiO_2 nanocrystals is suggested to facilitate an efficient electron−hole separation by attracting electrons.[49]

CONCLUSIONS

In conclusion, anatase TiO_2 nanosheets with varying {001} ratios have been investigated to understand the role of shape and surface morphology on photoactivity. An enhancement in photoactivity is observed for those with a {001} ratio of close to ~60%, which explains the shape effect. The subsequent NaOH (HF) treatments at room temperature are found to change the type and concentration of surface defects on TiO_2 in a way to enhance the photoactivity; interestingly enough, the enhancement is found to be quite pronounced, especially for species with a {001} ratio close to 60%. The detailed nature of surface defects is not simple, but EPR measurements give evidence that the surface defects favor the formation of surface O^- species under ambient conditions. The effect of surface F is found to be marginal in our case, which is attributed to the fact that the absolute F concentration is low. Instead, the overall enhancement in the photoactivity of our anatase TiO_2 nanocrystals is largely related to detailed surface conditions such as surface defects and morphology.

AUTHOR INFORMATION

Corresponding Author

*Y.K.K.: tel, 82-31-219-2896; fax, 82-31-219-2969; e-mail, yukwonkim@ajou.ac.kr.

Notes

The authors declare no competing financial interest.

ACKNOWLEDGMENTS

This research was supported by the Basic Science Research Program through the National Research Foundation of Korea (NRF) funded by the Ministry of Education, Science and Technology (NRF-2012R1A1A2007641).

REFERENCES

(1) Liu, G.; Yang, H. G.; Pan, J.; Yang, Y. Q.; Lu, G. Q.; Cheng, H.-M. *Chem. Rev.* **2014**, *114*, 9559−9612.
(2) Wang, L.; Sasaki, T. *Chem. Rev.* **2014**, *114*, 9455−9486.
(3) Chen, X.; Mao, S. S. *Chem. Rev.* **2007**, *107*, 2891−2959.
(4) Habas, S. E.; Lee, H.; Radmilovic, V.; Somorjai, G. A.; Yang, P. *Nat. Mater.* **2007**, *6*, 692−697.
(5) Liu, G.; Yu, J. C.; Lu, G. Q.; Cheng, H.-M. *Chem. Commun.* **2011**, *47*, 6763−6783.
(6) Zhou, W.; Liu, X.; Cui, J.; Liu, D.; Li, J.; Jiang, H.; Wang, J.; Liu, H. *CrystEngComm* **2011**, *13*, 4557−4563.
(7) Liu, G.; Yang, H. G.; Wang, X.; Cheng, L.; Lu, H.; Wang, L.; Lu, G. Q.; Cheng, H.-M. *J. Phys. Chem. C* **2009**, *113*, 21784−21788.
(8) Liu, S.; Yu, J.; Jaroniec, M. *J. Am. Chem. Soc.* **2010**, *132*, 11914−11916.
(9) Wu, B.; Guo, C.; Zheng, N.; Xie, Z.; Stucky, G. D. *J. Am. Chem. Soc.* **2008**, *130*, 17563−17567.
(10) Yu, J.; Fan, J.; Lv, K. *Nanoscale* **2010**, *2*, 2144−2149.
(11) Wen, C. Z.; Jiang, H. B.; Qiao, S. Z.; Yang, H. G.; Lu, G. Q. *J. Mater. Chem.* **2011**, *21*, 7052−7061.
(12) Wen, C. Z.; Zhou, J. Z.; Jiang, H. B.; Hu, Q. H.; Qiao, S. Z.; Yang, H. G. *Chem. Commun.* **2011**, *47*, 4400−4402.
(13) Wang, W.-S.; Wang, D.-H.; Qu, W.-G.; Lu, L.-Q.; Xu, A.-W. *J. Phys. Chem. C* **2012**, *116*, 19893−19901.
(14) Liu, S.; Yu, J.; Jaroniec, M. *Chem. Mater.* **2011**, *23*, 4085−4093.
(15) Yang, H. G.; Sun, C. H.; Qiao, S. Z.; Zou, J.; Liu, G.; Smith, S. C.; Cheng, H. M.; Lu, G. Q. *Nature* **2008**, *453*, 638−641.
(16) Yang, H. G.; Liu, G.; Qiao, S. Z.; Sun, C. H.; Jin, Y. G.; Smith, S. C.; Zou, J.; Cheng, H. M.; Lu, G. Q. *J. Am. Chem. Soc.* **2009**, *131*, 4078−4083.
(17) Han, X.; Kuang, Q.; Jin, M.; Xie, Z.; Zheng, L. *J. Am. Chem. Soc.* **2009**, *131*, 3152−3153.
(18) Zhang, D.; Li, G.; Wang, H.; Chan, K. M.; Yu, J. C. *Cryst. Growth Des.* **2010**, *10*, 1130−1137.
(19) Wang, Z.; Lv, K.; Wang, G.; Deng, K.; Tang, D. *Appl. Catal., B* **2010**, *100*, 378−385.
(20) Dai, Y.; Cobley, C. M.; Zeng, J.; Sun, Y.; Xia, Y. *Nano Lett.* **2009**, *9*, 2455−2459.
(21) Sosnowchik, B. D.; Heather, C. C.; Yong, D.; Jong-Yoon, H.; Zhong Lin, W.; Liwei, L. *Nanotechnology* **2010**, *21*, 485601.
(22) Li, J.; Xu, D. *Chem. Commun.* **2010**, *46*, 2301−2303.
(23) Yu, J.; Qi, L.; Jaroniec, M. *J. Phys. Chem. C* **2010**, *114*, 13118−13125.
(24) Liu, G.; Sun, C.; Yang, H. G.; Smith, S. C.; Wang, L.; Lu, G. Q.; Cheng, H.-M. *Chem. Commun.* **2010**, *46*, 755−757.
(25) Pan, J.; Liu, G.; Lu, G. Q.; Cheng, H.-M. *Angew. Chem., Int. Ed.* **2011**, *50*, 2133−2137.
(26) Xiang, Q.; Yu, J.; Jaroniec, M. *Chem. Commun.* **2011**, *47*, 4532−4534.
(27) Jiang, H. B.; Cuan, Q.; Wen, C. Z.; Xing, J.; Wu, D.; Gong, X.-Q.; Li, C.; Yang, H. G. *Angew. Chem., Int. Ed.* **2011**, *50*, 3764−3768.
(28) D'Arienzo, M.; Carbajo, J.; Bahamonde, A.; Crippa, M.; Polizzi, S.; Scotti, R.; Wahba, L.; Morazzoni, F. *J. Am. Chem. Soc.* **2011**, *133*, 17652−17661.
(29) Fang, W. Q.; Gong, X.-Q.; Yang, H. G. *J. Phys. Chem. Lett.* **2011**, *2*, 725−734.
(30) Wu, Q.; Liu, M.; Wu, Z.; Li, Y.; Piao, L. *J. Phys. Chem. C* **2012**, *116*, 26800−26804.
(31) Zuo, F.; Bozhilov, K.; Dillon, R. J.; Wang, L.; Smith, P.; Zhao, X.; Bardeen, C.; Feng, P. *Angew. Chem., Int. Ed.* **2012**, *51*, 6223−6226.
(32) Zhang, J.; Chen, W.; Xi, J.; Ji, Z. *Mater. Lett.* **2012**, *79*, 259−262.
(33) Wang, X.; He, H.; Chen, Y.; Zhao, J.; Zhang, X. *Appl. Surf. Sci.* **2012**, *258*, 5863−5868.
(34) Zhang, J.; Wang, J.; Zhao, Z.; Yu, T.; Feng, J.; Yuan, Y.; Tang, Z.; Liu, Y.; Li, Z.; Zou, Z. *Phys. Chem. Chem. Phys.* **2012**, *14*, 4763−4769.
(35) Ye, L.; Liu, J.; Tian, L.; Peng, T.; Zan, L. *Appl. Catal., B* **2013**, *134−135*, 60−65.

DOI: 10.1021/cs5020942
ACS Catal. 2015, 5, 3316−3322

(36) Xu, H.; Ouyang, S.; Li, P.; Kako, T.; Ye, J. *ACS Appl. Mater. Interfaces* **2013**, *5*, 1348−1354.
(37) Miao, J.; Liu, B. *RSC Adv.* **2013**, *3*, 1222−1226.
(38) Xu, H.; Reunchan, P.; Ouyang, S.; Tong, H.; Umezawa, N.; Kako, T.; Ye, J. *Chem. Mater.* **2013**, *25*, 405−411.
(39) Lai, Z.; Peng, F.; Wang, H.; Yu, H.; Zhang, S.; Zhao, H. *J. Mater. Chem. A* **2013**, *1*, 4182−4185.
(40) Selçuk, S.; Selloni, A. *J. Phys. Chem. C* **2013**, *117*, 6358−6362.
(41) Ong, W.-J.; Tan, L.-L.; Chai, S.-P.; Yong, S.-T.; Mohamed, A. R. *ChemSusChem* **2014**, *7*, 690−719.
(42) Lv, K.; Cheng, B.; Yu, J.; Liu, G. *Phys. Chem. Chem. Phys.* **2012**, *14*, 5349−5362.
(43) Zheng, Z.; Huang, B.; Lu, J.; Qin, X.; Zhang, X.; Dai, Y. *Chem. - Eur. J.* **2011**, *17*, 15032−15038.
(44) Wang, Q.; Chen, C.; Zhao, D.; Ma, W.; Zhao, J. *Langmuir* **2008**, *24*, 7338−7345.
(45) Yu, J.; Wang, W.; Cheng, B.; Su, B.-L. *J. Phys. Chem. C* **2009**, *113*, 6743−6750.
(46) Yu, J.; Low, J.; Xiao, W.; Zhou, P.; Jaroniec, M. *J. Am. Chem. Soc.* **2014**, *136*, 8839−8842.
(47) Liu, L.; Ji, Z.; Zou, W.; Gu, X.; Deng, Y.; Gao, F.; Tang, C.; Dong, L. *ACS Catal.* **2013**, *3*, 2052−2061.
(48) Kudo, A.; Miseki, Y. *Chem. Soc. Rev.* **2009**, *38*, 253−278.
(49) Yu, X.; Kim, B.; Kim, Y. K. *ACS Catal.* **2013**, *3*, 2479−2486.
(50) Tian, F.; Zhang, Y.; Zhang, J.; Pan, C. *J. Phys. Chem. C* **2012**, *116*, 7515−7519.
(51) Xiang, Q.; Lv, K.; Yu, J. *Appl. Catal., B* **2010**, *96*, 557−564.
(52) Liu, M.; Piao, L.; Zhao, L.; Ju, S.; Yan, Z.; He, T.; Zhou, C.; Wang, W. *Chem. Commun.* **2010**, *46*, 1664−1666.
(53) Tsai, C.-C.; Teng, H. *Chem. Mater.* **2006**, *18*, 367−373.
(54) Kitano, M.; Iyatani, K.; Tsujimaru, K.; Matsuoka, M.; Takeuchi, M.; Ueshima, M.; Thomas, J. M.; Anpo, M. *Top. Catal.* **2008**, *49*, 24−31.
(55) Czoska, A. M.; Livraghi, S.; Chiesa, M.; Giamello, E.; Agnoli, S.; Granozzi, G.; Finazzi, E.; Valentin, C. D.; Pacchioni, G. *J. Phys. Chem. C* **2008**, *112*, 8951−8956.
(56) Dozzi, M. V.; Ohtani, B.; Selli, E. *Phys. Chem. Chem. Phys.* **2011**, *13*, 18217−18227.
(57) Zuo, F.; Wang, L.; Wu, T.; Zhang, Z.; Borchardt, D.; Feng, P. *J. Am. Chem. Soc.* **2010**, *132*, 11856−11857.
(58) Strunk, J.; Vining, W. C.; Bell, A. T. *J. Phys. Chem. C* **2010**, *114*, 16937−16945.
(59) Wei, W.; Yaru, N.; Chunhua, L.; Zhongzi, X. *RSC Adv.* **2012**, *2*, 8286−8288.
(60) Wang, W.; Lu, C.; Ni, Y.; Su, M.; Xu, Z. *Appl. Catal., B* **2012**, *127*, 28−35.

DOI: 10.1021/cs5020942
ACS Catal. 2015, 5, 3316−3322